

COVER PAGE

Document downloaded by @DAEL

Sun Nov 29 15:53:10 2026
For personal use

When automatic English translation is provided, only the original document is authentic.
The EAA cannot be held responsible of any translation error

Bibliographical reference

Reflection and Transmission of Sound From a Dipole Source Near a Rigid Porous Medium, K. M. Li and H. Tao, Acta Acustica **vol. 99** (Number 5), 2013, pp. 703-715

DOI
https://doi.org/10.3813/AAA.918649

Acta Acustica united with Acustica
Vol. 99 (2013) 703 – 715

DOI 10.3813/AAA.918649

Reflection and Transmission of Sound From a Dipole Source Near a Rigid Porous Medium

K. M. Li, H. Tao
Ray W. Herrick Laboratories, School of Mechanical Engineering, Purdue University, 140 S. Martin Jischke Drive, West Lafayette, IN 47907-2031, U.S.A. mmkli@purdue.edu

Summary
An asymptotic analysis has been conducted to examine the sound fields due to an arbitrarily oriented dipole that is placed above a rigid porous medium. In the study, the diffraction of sound owing to the effect of spherical wavefronts and the presence of the porous interface has been explored. By using a double saddle point analysis supplemented by the pole subtraction method, the asymptotic solutions for the dipole sound fields reflected from and transmitted through the porous interface have been derived. The diffracted wave contributions in both situations can be expressed conveniently in terms of a standard complementary error function that can be computed efficiently. By using these asymptotic formulas, the total sound fields in the vicinity of a rigid porous medium can be calculated accurately and rapidly.

PACS no. 43.20.Bi, 43.20.El, 43.28.En, 43.28.Hr, 43.28.Js

1. Introduction

The reflection of sound from a porous half-space has been the subject of interest for many decades [1, 2, 3, 4, 5, 6, 7]. There have also been related studies on the transmission of sound through an interface into a porous half-space. An application of these studies is the acoustic detection of buried objects [8, 9, 10, 11]. Most of these studies were based on the sound fields generated by a point monopole source. Other studies considered a directional noise source but these were mainly restricted to the analysis of sound fields above a locally reacting ground [12, 13, 14, 15].

The purpose of this study is to develop accurate numerical solutions for predicting the sound fields above and below a porous half-space due to a dipole source placed above the interface since many noise sources have directional characteristics. For instance, a fast moving train [16] and a helicopter rotor [17] can be modeled as dipole noise sources. The analytical and numerical solutions developed in this paper will be beneficial in the accurate assessment of the noise impacts from directional sources. It should be pointed out that there were comparable studies on the propagation of electromagnetic waves over a conducting half-plane due to an electric dipole in recent decades (e.g. [18, 19, 20]). However, these analytical results cannot be applied directly without further adaptations to most acoustic problems.

Indeed, the problem of predicting the sound fields due to a point monopole source above a plane interface, and also the related problem for a dipole source, is of great theoretical interest. It is because they can be posed as an exactly solvable canonical problem with a rich structure. Their analytical solutions are also of considerable practical importance in, for instance, the implementation of noise mapping software. There are many exact computational schemes, such as the fast field program [21], finite element method [22], offering accurate numerical solutions for predicting sound fields for the canonical problems. However, the computational costs of these numerical schemes are prohibitively expensive for high source frequencies. These numerical solutions do not yield physically interpretable terms to enhance a better understanding of the problem. An alternative route is pursued in the present study where an asymptotic method is applied to derive an approximate solution for the dipole sound fields of the classical two- medium problem. Previous studies [6, 7, 23, 24, 25] have shown that the method of steepest descent is a versatile mathematical technique that offers accurate and fast asymptotic solutions for computation of sound fields above a flat interface. The present study generalizes this mathematical technique to tackle the problem of the sound field due to a dipole source placed above a rigid porous medium.

Another application of the present study is its provision of an accurate Green's function that can be used to calculate the pressure gradient at any arbitrary field point above a rigid porous ground. Accurate Green's functions for calculating the pressure and the pressure gradients are normally required in the boundary integral equation (BIE) formulation for predicting the combined effects of a porous road surface and the application of sound absorbing materials on a barrier's surface. In the absence of appropriate Green's functions, Anfosso-Ledee *et al.* [26]

Received 16 May 2012,
accepted 26 June 2013.

© S. Hirzel Verlag · EAA

used a two-domain BIE approach to impose the continuity of pressure and velocity at the porous interface. Their BIE approach invariably increases the number of elements needed in the formulations, which limits its suitability as a three-dimensional boundary element model. On the other hand, an analytical solution below ground facilitates the acoustical characterization of sound absorbing materials and has an application in the acoustic detection of buried objects by means of a BIE formulation [9].

It is well known that the sound field above a rigid porous medium consists of three terms: a direct wave, a reflected wave, and a component due to sound diffracted at the interface. In a recent study, Li and Liu [6] showed that the sound field below the porous interface consists of two terms: a sound transmission component and a diffracted wave term. This paper reports a continuation of these efforts to develop asymptotic formulas for predicting the sound field above and below a rigid porous medium. A double saddle point method [24] will be used to evaluate the diffraction integral along the steepest descent path. The method of pole subtraction is then applied to provide a uniform asymptotic solution for the sound fields above and below the porous interface. In this paper, we shall interpret the directional effect of the dipole source on each term of the asymptotic solutions. The accuracy of the asymptotic solutions will be confirmed by comparing them with computationally intensive, but more accurate, numerical schemes.

2. Review of the diffraction integrals for a monopole source placed above a rigid porous medium

A rectangular coordinate system is used with the vertical z-axis passing through the source, i.e., the coordinate of the source is $(0, 0, z_s)$. The frequency of the dipole source is f, the corresponding wave number is k, and the speed of sound in air (upper medium) is c. A receiver is placed at z above the porous interface where the height z is measured positive upward. Alternatively, the receiver may be placed at a depth $-D$ below the interface where $D > 0$. A horizontal coordinate of $\boldsymbol{r} = (x, y)$ is used where its scalar horizontal distance from the source is $r = \sqrt{x^2 + y^2}$ and the corresponding azimuthal angle is $\psi = \arctan(y/x)$. The parameters R_1 and R_2 are defined as the respective distances from the source and its image to the receiver, i.e., the distances of the direct and reflected waves. The ground is assumed to have a complex sound speed and complex density of c_1 and ρ_1, respectively. Figure 1a shows the geometrical configuration of the present study.

According to a recent study, Li and Liu [7] showed that the sound fields above (at height of $z > 0$) and below (at depth of $D > 0$) the porous interface can be expressed as

$$p^{(m)}(r, z_s, z) = \frac{\mathrm{e}^{\mathrm{i}kR_1}}{4\pi R_1} + \frac{\mathrm{e}^{\mathrm{i}kR_2}}{4\pi R_2} + p_a^{(m)} \tag{1a}$$

and

$$p^{(m)}(r, z_s, -D) = p_b^{(m)}, \tag{1b}$$

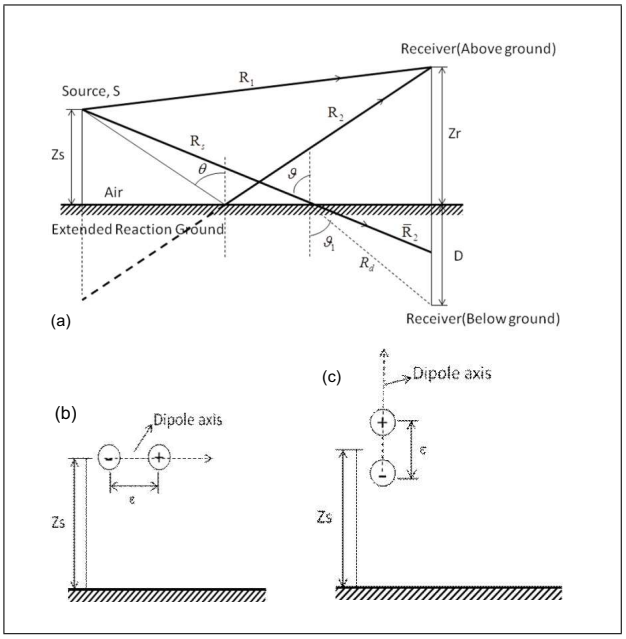


Figure 1. (a) Schematic diagram showing a source located in the air in the upper medium, a receiver situated at height z_r above the interface, and another receiver located at depth D below the incident angle for the refracted ray, and ϑ_1 is the refracted angle. The distance R_s is measured from the source to the ground and $\overline{R}_2$ is measured from the source to the apparent receiver below the ground. The schematic diagrams of dipole sources are shown in (b) a horizontal dipole, and (c) a vertical dipole. A pair of monopole sources of opposite signs are aligned accordingly and placed at a height of z_s above the rigid porous medium.

where $p^{(m)}$ $[\equiv p_a^{(m)}(r, z_s, z)]$ and $p_b^{(m)}$ $[\equiv p_b^{(m)}(r, z_s, D)]$ are the respective integrals to calculate the contribution of the diffracted wave terms above and below the porous interface. The superscript (m) represents the sound field due to a monopole source i.e., a zeroth order multipole. Li and Liu showed that the diffraction integrals due to a monopole source can be written as

$$p_a^{(m)}(r, z_s, z) = \frac{-\mathrm{i}k}{4\pi} \int_C \frac{\zeta\sqrt{n^2 - \sin^2\mu}\,\sin\mu\, G_0(\mu)\exp[\mathrm{i}k f_a(\mu)]}{\cos\mu + \zeta\sqrt{n^2 - \sin^2\mu}}\mathrm{d}\mu \tag{2a}$$

and

$$p_b^{(m)}(r, z_s, D) = \frac{\mathrm{i}k}{4\pi} \int_C \frac{\cos\mu\sin\mu\, G_0(\mu)\exp[\mathrm{i}k f_b(\mu)]}{\cos\mu + \zeta\sqrt{n^2 - \sin^2\mu}}\mathrm{d}\mu, \tag{2b}$$

where $\zeta = \rho/\rho_1$ is the complex density ratio, $n = c/c_1$ is the index of refraction from the upper medium to the lower medium, and $G_j(\mu)$ (where $j = 0, 1, \ldots$), is the corresponding jth order Hankel function $H_j^{(1)}$ normalized with the exponential factor $\mathrm{e}^{-\mathrm{i}kr\sin\mu}$,

$$G_j(\mu) = H_j^{(1)}\left(kr\sin\mu\right)\mathrm{e}^{-\mathrm{i}kr\sin\mu}. \tag{3a}$$

The asymptotic form for $G_j(\mu)$ can be expressed as [27]

$$G_j(\mu) \approx (-\mathrm{i})^j \sqrt{\frac{2}{\mathrm{i}\pi kr \sin\mu}} \left[1 - \frac{4\mathrm{j}^2 - 1}{8\mathrm{i}kr \sin\mu} + \ldots\right]. \quad (3b)$$

Here, j is set to zero for a monopole source. The variable μ in the diffraction integrals can be interpreted as the angle of incidence of the reflected plane wave [25] in the upper medium. The exponential factor $f_a(\mu)$ in equation (2a) and $f_b(\mu)$ in equation (2b) are defined, respectively, by

$$f_a(\mu) = r \sin\mu + (z_s + z)\cos\mu = R_2 \cos(\mu - \theta) \quad (4a)$$

and

$$f_b(\mu) = r \sin\mu + z_s \cos\mu + D\sqrt{n^2 - \sin^2\mu}, \quad (4b)$$

where $z_s, z, D \geq 0$.

The integration path for the two diffraction integrals is shown as C in Figure 2. The integration path for μ varies from $-\pi/2 + \mathrm{i}\infty$ to $-\pi/2$ to $\pi/2$ to $\pi/2 - \mathrm{i}\infty$. It is remarkable that the pole μ_p is the same for both integrands shown in equations (2a) and (2b). It can be determined by setting the denominators of the respective integrands to zero, i.e. $\cos\mu + \zeta\sqrt{n^2 - \sin^2\mu} = 0$. Its solution gives a pair of trigonometrical functions defining its location at the complex μ-plane as

$$\cos\mu_p = -\zeta\sqrt{(n^2 - 1)/(1 - \zeta^2)} = -\beta_p \quad (5a)$$

and

$$\sin\mu_p = \sqrt{(1 - \zeta^2 n^2)/(1 - \zeta^2)} = \sqrt{1 - \beta_p^2}, \quad (5b)$$

where the subscript p stands for the parameter at the pole. Figure 2 also shows the schematic location of the pole in the complex μ-plane. The term β_p, which is introduced in equations (5a) and (5b), can be treated as the apparent admittance of the rigid porous medium.

It should be pointed out that accurate asymptotic solutions [7] were available to compute the diffraction integrals, $p_a^{(m)}$ and $p_b^{(m)}$. In principle, the dipole sound fields could be obtained directly by taking directional derivatives of these asymptotic solutions. However, the spatial derivatives of the diffraction integral lead to more complex expressions [18]. A preliminary analysis suggests that this direct approach leads to a set of complicated asymptotic solutions which is tedious to apply for computing the dipole sound fields. We are therefore refrained from providing the approximate solutions due to a monopole source in this section. The diffraction integrals described above will be used instead as a basis for the derivation of the dipole sound fields in the following sections.

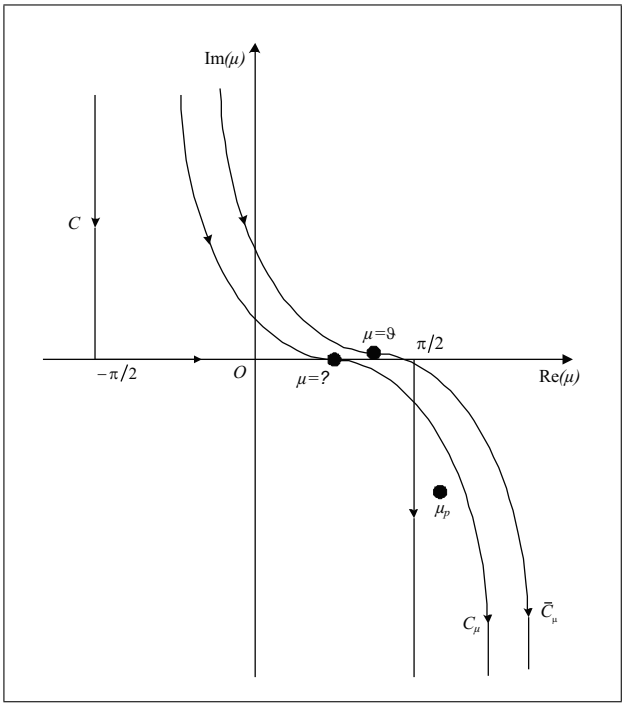


Figure 2. Sketch of the integration paths. The original integration path is denoted by C, whereas C_μ and $\overline{C}_\mu$ are the steepest descent paths for the sound fields above and below the rigid porous ground, respectively.

3. Dipole sound fields above a rigid porous medium

3.1. Integral expressions for the diffracted wave term

Suppose a dipole is placed at a height of z_s above a semi-infinite plane interface. Figures 1b and 1c show schematic diagrams for a horizontal dipole and a vertical dipole. The dipole sources may be considered as a pair of opposite monopole sources separated by a small distance ε (where $\varepsilon \to 0$) along the dipole axis.

The dipole axis is specified by the polar and azimuthal angles (γ_L and ψ_L). The direction cosines $\boldsymbol{l} = (l_x, l_y, l_z)$ of the dipole axis can be specified by

$$l_x = \sin\gamma_L \cos\psi_L, \quad l_y = \sin\gamma_L \sin\psi_L, \quad l_z = \cos\gamma_L. \quad (6)$$

The horizontal and vertical components for the dipole orientation are introduced such that $\boldsymbol{l} = (\boldsymbol{l}_h, \boldsymbol{l}_v)$, where $\boldsymbol{l}_h = (l_x, l_y)$ and $\boldsymbol{l}_v = (l_z)$. The use of these two components can simplify the expression given in our analytical solution. It is because the two planar direction cosines, l_x and l_y, can be grouped together as a single term for the sound field due to the horizontal dipoles. On the other hand, the polar direction cosine l_z gives rise to the contribution due to the vertical dipole. Unless stated otherwise, the subscripts h and v are used to denote the horizontal and vertical components of the variable.

Taking directional derivatives [6], the sound fields due to an arbitrarily oriented dipole source can be written in

terms of $p^{(m)}$ as

$$p^{(d)}(r, z_s, z) = \\ - \left[\sin\gamma_L \cos(\psi - \psi_L)\partial_r + \cos\gamma_L \partial_z\right] p^{(m)}(r, z_s, z), \tag{7}$$

where r and ψ are the magnitude and direction of the receiver in the azimuthal plane. The superscripts (d) and (m) represent the parameters for a dipole source (i.e., the first order multi-pole) and a monopole source (i.e., the zero order multi-pole) respectively. The subscripts r and z in ∂ represent the spatial derivatives $\partial/\partial r$ and $\partial/\partial z$, respectively. Differentiation the first two terms of equation (1a) with respect to r and z, substitution of the resulting expressions into equation (7) and manipulation of the algebraic terms lead to

$$p^{(d)}(r, z_s, z) = \left(\boldsymbol{l}\cdot\boldsymbol{u}_1\right)\left[\frac{1 - \mathrm{i}kR_1}{4\pi R_1^2}\right]\mathrm{e}^{\mathrm{i}kR_1} \\ + \left(\boldsymbol{l}\cdot\boldsymbol{u}_2\right)\left[\frac{1 - \mathrm{i}kR_2}{4\pi R_2^2}\right]\mathrm{e}^{\mathrm{i}kR_2} + p_a^{(d)}, \tag{8a}$$

where the diffracted wave term $p_a^{(d)}$ is given by

$$p_a^{(d)} = -\left[\sin\gamma_L \cos(\psi - \psi_L)\partial_r + \cos\gamma_L \partial_z\right] p_a^{(m)}, \tag{8b}$$

and the unit vectors $\boldsymbol{u}_1$ and $\boldsymbol{u}_2$ are the respective directions pointing from the source and its image to the receiver. Centering at the source and image source, $\boldsymbol{u}_1$ and $\boldsymbol{u}_2$ can be written in terms of the polar and azimuthal angles as

$$\boldsymbol{u}_1 = \left(\sin\phi\cos\psi, \sin\phi\sin\psi, \cos\phi\right) \tag{9a}$$

and

$$\boldsymbol{u}_2 = \left(\sin\theta\cos\psi, \sin\theta\sin\psi, \cos\theta\right), \tag{9b}$$

where ϕ and θ are the respective polar angles of the direct and reflected waves, and ψ is the azimuthal angle for both the direct and reflected wave.

We can see that the diffracted wave term for the dipole $p_a^{(d)}$ can also be split into its horizontal and vertical components. Straightforward directional derivatives of the asymptotic solution for $p_a^{(m)}$ in equation (8b) will result in a more complicated asymptotic solution [13]. Here, we shall take an alternative approach by reversing the order of differentiation and integration for $\partial_r p_a^{(m)}$ and $\partial_z p_a^{(m)}$ to yield

$$\partial_r p_a^{(m)} = \frac{\partial p_a^{(m)}}{\partial r} \\ = \frac{\mathrm{i}k^2}{4\pi}\int_C \frac{\zeta \sin^2\mu\sqrt{n^2 - \sin^2\mu}\, G_1(\mu)\mathrm{e}^{\mathrm{i}kf_a(\mu)}}{\cos\mu + \zeta\sqrt{n^2 - \sin^2\mu}}\mathrm{d}\mu \tag{10a}$$

and

$$\partial_z p_a^{(m)} = \frac{\partial p_a^{(m)}}{\partial z} \\ = \frac{k^2}{4\pi}\int_C \frac{\zeta \cos\mu \sin\mu\sqrt{n^2 - \sin^2\mu}\, G_0(\mu)\mathrm{e}^{\mathrm{i}kf_a(\mu)}}{\cos\mu + \zeta\sqrt{n^2 - \sin^2\mu}}\mathrm{d}\mu, \tag{10b}$$

where $G_j(\mu)$ (where $j = 0, 1, \ldots$) is defined by equations (3a,b) and the exponential function f_a above the rigid porous medium is given by equation (4a).

It is important to mention that the diffracted sound fields above a rigid porous medium due to the horizontal and vertical dipoles can be obtained from equations (10a) and (10b). In the special case where $n \to \infty$, i.e., a locally reacting ground, these integral expressions can be reduced to the analogous forms given by Li *et al.* [13] which can be evaluated asymptotically leading to a closed form solution. However, to the best of our knowledge, the corresponding asymptotic solutions are not available for the arbitrarily oriented dipole. One of the objectives of the present study is to derive such asymptotic formulas for providing fast and accurate numerical solutions to predict the dipole sound fields above a rigid porous medium. The details of the derivation will be given in the following sections.

3.2. Diffracted wave fields due to a horizontal dipole

In this section, an analytical method [6] will be used to derive an asymptotic solution for the horizontal dipole $\partial_r p_a^{(m)}$. The corresponding solution for the vertical dipole $\partial_r p_a^{(m)}$ will be discussed in the next section. The sum of these two solutions, $\partial_r p_a^{(m)}$ and $\partial_z p_a^{(m)}$, leads to an analytical formula for the diffracted wave term due to an arbitrarily oriented dipole.

The main steps for evaluating the integrals asymptotically are described for the sake of completeness. First, the integration path C is deformed to the steepest descent path C_μ (see Figure 1) that passes through the saddle point at $\mu = \theta$. The steepest descent path can then be determined by setting

$$\Im m\left\{\mathrm{i}\left[1 - \cos(\mu - \theta)\right]\right\} = 0. \tag{11}$$

Figure 2 shows both integration paths in the complex μ-plane.

By indenting the path from C to C_μ, the contribution from the pole is included, which yields an expression for $\partial_r p_a^{(m)}$ as

$$\partial_r p_a^{(m)} = \frac{\mathrm{i}k^2}{4\pi}\int_{C_\mu} \frac{\zeta N(\mu)\sin^2\mu\, G_1(\mu)\,\mathrm{e}^{\mathrm{i}kR_2\cos(\mu-\theta)}}{\cos\mu + \zeta N(\mu)}\mathrm{d}\mu \\ + H\left[\Im m\left\{\mathrm{i}\left[1 - \cos(\mu - \theta)\right]\right\}\right] p_h^{(d)}, \tag{12a}$$

where H is the Heaviside step function and $p_h^{(d)}$ is the pole contribution that can be determined by the calculus of residue to confirm

$$p_h^{(d)} = \frac{k^2\zeta N(\mu_p)\sin\mu_p H_1^{(1)}(kr\sin\mu_p)\,\mathrm{e}^{\mathrm{i}k(z_s+z)\cos\mu_p}}{2(1 - \zeta^2)}. \tag{12b}$$

The evaluation of the integral in equation (12a) is facilitated by introducing a complex variable W to replace μ by

$$\frac{1}{2}W^2 = \mathrm{i}kR_2\left[1 - \cos(\mu - \theta)\right]. \tag{13a}$$

The pole location W_p in the W-plane can then be determined, but it is usually written in terms of the numerical distance w as

$$w = W_p/\sqrt{2} = \sqrt{2\mathrm{i}kR_2}\sin\big[(\mu_p-\theta)/2\big]. \quad (13b)$$

Because the steepest descent path in the W-plane corresponds to the integration path along its real axis, equation (12a) can therefore be transformed to

$$\partial_r p_a^{(m)} = I_1 + H\big[-\Im m\{W_p\}\big]p_h^{(d)}, \quad (14a)$$

where

$$I_1 = \frac{\mathrm{i}k^2}{4\pi}\mathrm{e}^{\mathrm{i}kR_2}\int_{-\infty}^{\infty}\varpi_h^{(1)}\mathrm{e}^{-X^2/2}\mathrm{d}X, \quad (14b)$$

$$\varpi_h^{(1)}(X) = \frac{\zeta N(\mu)\sin^2\mu\, G_1(\mu)}{\big[\cos\mu+\zeta N(\mu)\big]\sqrt{\mathrm{i}kR_2 - X^2/4}}, \quad (14c)$$

$X = \Re e\{W\}$, and μ can be converted to W according to equation (13a).

Essentially, the method of pole subtraction is needed when the pole μ_p is positioned very close to the saddle point θ, i.e., when W_p is very close to 0. In this case, the apparent singularity of the integrand in equation (12a) can be removed by the method of pole subtraction [24]. Specifically, equation (12a) can be rewritten as

$$\partial_r p_a^{(m)} = I_2 + H\big[-\Im m\{W_p\}\big]p_h^{(d)} + \phi_h^{(d)}, \quad (15a)$$

where

$$I_2 = \frac{\mathrm{i}k^2}{4\pi}\mathrm{e}^{\mathrm{i}kR_2}\int_{-\infty}^{\infty}\Theta_h^{(1)}(X)\mathrm{e}^{-X^2/2}\mathrm{d}X, \quad (15b)$$

$$\Theta_h^{(d)}(X) = -\frac{\zeta N(\mu_p)\sin\mu_p\, G_1(\mu_p)}{(1-\zeta^2)(X-W_p)}, \quad (15c)$$

and

$$\begin{aligned}\phi_h^{(d)} &= I_1 - I_2 \quad (15d)\\ &= \frac{\mathrm{i}k^2}{4\pi}\mathrm{e}^{\mathrm{i}kR_2}\int_{-\infty}^{\infty}\big[\varpi_h^{(d)} - \Theta_h^{(1)}(X)\big]\mathrm{e}^{-X^2/2}\mathrm{d}X.\end{aligned}$$

By noting $p_h^{(d)}$ in equation (12b), an asymptotic expression for G_1 (see equation 3b) in equation (15c), and, an integral expression for the complementary error function [27],

$$\begin{aligned}&\int_{-\infty}^{\infty}\frac{\mathrm{e}^{-X^2/2}}{X-\sqrt{2}w}\mathrm{d}X \quad (16)\\ &= -\frac{\pi}{\mathrm{i}}\mathrm{e}^{-w^2}\big[\mathrm{erfc}(-\mathrm{i}w) - 2H\big(-\Im m\{w\}\big)\big],\end{aligned}$$

the integral I_2 can be simplified to confirm

$$I_2 = \big(\mathrm{i}k\Xi\sin\mu_p\big)\frac{\mathrm{e}^{\mathrm{i}kR_2}}{4\pi R_2} - H\big(-\Im m\{w\}\big)p_h^{(d)}, \quad (17)$$

where Ξ is defined in terms of the complimentary error function as

$$\Xi = 2\mathrm{i}\sqrt{\pi}\sqrt{\mathrm{i}kR_2/2}\frac{\beta_p\mathrm{e}^{-w^2}\,\mathrm{erfc}(-\mathrm{i}w)}{(1-\zeta^2)\sqrt{\sin\theta\sin\mu_p}}. \quad (18)$$

The application of the Taylor's series expansion to the integrand of equation (14b), retention of the first term in the series, and, evaluation of the resulting integral yield a closed form asymptotic solution for I_1 as

$$I_1 = \mathrm{i}k\phi_A\sin\theta\frac{\mathrm{e}^{\mathrm{i}kR_2}}{4\pi R_2}, \quad (19)$$

where ϕ_A is given by

$$\phi_A \approx \frac{-2\beta_e}{\cos\theta+\beta_e}, \quad (20a)$$

and

$$\beta_e = \zeta\sqrt{n^2-\sin^2\theta}. \quad (20b)$$

The asymptotic representation for I_2 can be derived using the following asymptotic formula for the complimentary error function,

$$\begin{aligned}&\mathrm{e}^{-W_p^2/2}\big[\mathrm{erfc}(-\mathrm{i}W_p/\sqrt{2}) - 2H\big(-\Im m\{W_p\}\big)\big]\\ &\qquad = \frac{1}{-\mathrm{i}W_p\sqrt{\pi/2}}\Big[1+\frac{1}{W_p^2}+\ldots\Big]. \quad (21)\end{aligned}$$

The substitution of equation (21) into equation (17) yields

$$I_2 = \mathrm{i}k\phi_B\sin\mu_p\frac{\mathrm{e}^{\mathrm{i}kR_2}}{4\pi R_2}, \quad (22a)$$

where ϕ_B is given by

$$\phi_B \approx \frac{-2\beta_p/\sqrt{2\sin\theta\sin\mu_p}}{(1-\zeta^2)\sqrt{1-\cos(\mu_p-\theta)}}. \quad (22b)$$

The subtraction of I_2 from I_1 leads to an asymptotic expression for the correction term as

$$\phi_h^{(d)} = \big[\big(\mathrm{i}k\sin\theta\big)\phi_A - \big(\mathrm{i}k\sin\mu_p\big)\phi_B\big]\frac{\mathrm{e}^{\mathrm{i}kR_2}}{4\pi R_2}. \quad (23)$$

This is the correction term that has been modified to take into account a spatial derivative with respect to r for the horizontal dipole. Namely, the multiplication factors of $(\mathrm{i}k\sin\theta)$ and $(\mathrm{i}k\sin\mu_p)$ appear in the first and the second term of the square bracket of equation (23), respectively. Substituting equations (17) and (23) into equation (15a), an asymptotic expression to calculate $\partial_r p_a^{(m)}$ can be obtained to confirm

$$\partial_r p_a^{(m)} = \mathrm{i}k\big[\phi_A\sin\theta + \mathrm{Y}_a\sin\mu_p\big]\frac{\mathrm{e}^{\mathrm{i}kR_2}}{4\pi R_2}, \quad (24a)$$

where the correction term, Y_a, is referred as the diffraction factor,

$$\begin{aligned}\mathrm{Y}_a &= \Xi - \phi_B \quad (24b)\\ &= \frac{2\beta_p}{(1-\zeta^2)\sqrt{\sin\theta\sin\mu_p}}\Big\{\big[2/1-\cos(\mu_p-\theta)\big)\big]^{-1/2}\\ &\quad + \mathrm{i}\sqrt{\pi}\sqrt{\mathrm{i}kR_2/2}\,\mathrm{e}^{-w^2}\,\mathrm{erfc}(-\mathrm{i}w)\Big\}.\end{aligned}$$

3.3. Diffracted wave fields due to a vertical dipole

In this section, the derivation of an asymptotic solution for the diffracted wave term due to a vertical dipole, $\partial_z p_a^{(m)}$, will be shown. Its exact solution can be specified in an integral form, as shown in equation (10b). By indenting the integration path from C to C_μ (see Figure 2), splitting the integral into two parts, replacing μ with W according to equation (13a), and evaluating the integral along the steepest descent path (i.e., along the real axis of W), the integral solution for $\partial_z p_a^{(m)}$ can be transformed into

$$\partial_z p_a^{(m)} = I_A + I_B, \tag{25a}$$

where

$$I_A = \frac{k^2}{4\pi} \mathrm{e}^{\mathrm{i}kR_2} \int_{-\infty}^{\infty} \frac{\zeta N(\mu) \sin\mu\, G_0(\mu)\, \mathrm{e}^{-X^2/2}}{\sqrt{\mathrm{i}kR_2 - X^2/4}} \mathrm{d}X, \tag{25b}$$

$$I_B = I_3 + H\big(-\Im m\{W_p\}\big) P_v^{(d)}, \tag{25c}$$

$$I_3 = -\frac{k^2}{4\pi} \mathrm{e}^{\mathrm{i}kR_2} \int_{-\infty}^{\infty} \varpi_v^{(d)}\, \mathrm{e}^{-X^2/2} \mathrm{d}X, \tag{26a}$$

$$\varpi_h^{(1)}(X) = \frac{\zeta^2 N^2(\mu) \sin\mu\, G_0(\mu)}{\big[\cos\mu + \zeta N(\mu)\big]\sqrt{\mathrm{i}kR_2 - X^2/4}}, \tag{26b}$$

$$P_v^{(d)} = \mathrm{i}k\beta_p \frac{k}{2} \frac{\beta_p G_0(\mu_p)}{1-\zeta^2} \mathrm{e}^{\mathrm{i}kR_2} \mathrm{e}^{-W_p^2/2} \tag{26c}$$

When deforming the integration path from C to C_μ, the contributions from the poles are required. Because the integrand of the first term in equation (25a) is an entire function (see also equation 25b), there is no pole contribution from this term. The integral I_A can therefore be evaluated asymptotically to yield

$$I_A = -\mathrm{i}k\beta_e \frac{\mathrm{e}^{\mathrm{i}kR_2}}{2\pi R_2}. \tag{27}$$

However, there is a pole in the second term of equation (25a), see also equations (25c), (26a) and $\varpi_v^{(1)}(X)$ in equation (26b). Hence, the pole contribution is calculated by the second term of equation (25c). It can be determined by using the same method as described in the last section to give an analytical expression for $p_v^{(1)}$ shown in equation (26c).

Using the same procedure as detailed in the last section, I3 can be evaluated by the pole subtraction method to verify

$$I_B = I_4 + H\big(-\Im m\{W_p\}\big) P_v^{(d)} + \phi_v^{(d)}, \tag{28}$$

where

$$I_4 = -\frac{k^2}{4\pi} \mathrm{e}^{\mathrm{i}kR_2} \int_{-\infty}^{\infty} \Theta_v^{(d)}(X)\, \mathrm{e}^{-X^2/2} \mathrm{d}X, \tag{29a}$$

$$\Theta_v^{(d)}(X) = -\frac{\zeta^2 N^2(\mu)\, G_0(\mu_p)}{(1-\zeta^2)(X - W_p)}, \tag{29b}$$

and

$$\begin{aligned} \phi_v^{(d)} &= I_3 - I_4 \\ &= -\frac{k^2}{4\pi} \mathrm{e}^{\mathrm{i}kR_2} \int_{-\infty}^{\infty} \big[\varpi_v^{(d)} - \Theta_v^{(1)}(X)\big]\, \mathrm{e}^{-X^2/2} \mathrm{d}X. \end{aligned} \tag{29c}$$

Using equation (17), the integral I4 can be represented exactly in terms of Ξ, cf. equation (18), to give

$$I_4 = (\mathrm{i}k\Xi\cos\mu_p) \frac{\mathrm{e}^{\mathrm{i}kR_2}}{4\pi R_2} - H\big(-\Im m\{W_p\}\big) P_v^{(d)}. \tag{30a}$$

The asymptotic solution for I_3 can be derived by a straightforward application of asymptotic analysis to give

$$I_3 = (\mathrm{i}k\phi_A \cos\theta_e) \frac{\mathrm{e}^{\mathrm{i}kR_2}}{4\pi R_2}, \tag{30b}$$

where θ_e is defined in an analogous form as the pole location θ_p as

$$\cos\theta_e + \beta_e = 0, \tag{30c}$$

with β_e defined in equation (20b). The asymptotic representation of I_4 can be obtained readily by using equation (21) to yield

$$I_4 = (\mathrm{i}k\phi_B \cos\mu_p) \frac{\mathrm{e}^{\mathrm{i}kR_2}}{4\pi R_2}, \tag{31}$$

where ϕ_B is defined in equation (22b). Hence, the substitution of equations (30b) and (31) into equation (29c) yields an asymptotic expression for the correction term as

$$\phi_v^{(d)} = \big[(\mathrm{i}k\cos\theta_e)\phi_A - (\mathrm{i}k\cos\mu_p)\phi_B\big] \frac{\mathrm{e}^{\mathrm{i}kR_2}}{4\pi R_2}. \tag{32}$$

Finally, the diffracted wave term above a rigid porous medium, due to a vertical dipole can be derived by first substituting equation (32) into equation (28). Then, the resulting asymptotic expressions for I_A and I_B (cf. equations 27 and 28) are used in equations (25a) to obtain

$$\partial_z p_a^{(m)} = \mathrm{i}k\big[(2+\phi_A)\cos\theta_e + \Upsilon_a \cos\mu_p\big] \frac{\mathrm{e}^{\mathrm{i}kR_2}}{4\pi R_2}, \tag{33}$$

where ϕ_A and Υ_a are given respectively by equation (20a) and equation (24b).

3.4. Sound fields due to an arbitrarily oriented dipole

For an arbitrarily oriented dipole with its dipole axis aligned according to equation (6), the diffracted wave term can be obtained by substituting equations (24a) and (33) into equation (8b) to verify

$$\begin{aligned} p_a^{(d)} = -\mathrm{i}k\big[&\big(\phi_A \sin\theta \sin\gamma_L \cos(\psi - \psi_L) \\ &+ (2+\phi_A)\cos\theta_s \cos\gamma_L\big) \\ &+ \Upsilon_a\big(\sin\gamma_L \cos(\psi - \psi_L) + \cos\gamma_L\big)\big] \frac{\mathrm{e}^{\mathrm{i}kR_2}}{4\pi R_2}. \end{aligned} \tag{34}$$

Using the spatial unit vectors $\boldsymbol{l}$ and $\boldsymbol{u}_2$ (see equations 6 and 9b) and introducing a unit vector $\boldsymbol{u}_s$ that characterizes the propagation direction of the boundary wave, equation (34) can be written in a more compact form as

$$p_a^{(d)} \approx \big(\boldsymbol{l}\cdot\boldsymbol{u}_2\big)\phi_A\Big[\frac{1-\mathrm{i}kR_2}{4\pi R_2^2}\Big]\,\mathrm{e}^{\mathrm{i}kR_2} + \big(\boldsymbol{l}\cdot\boldsymbol{u}_s\big)\mathrm{Y}_a\Big[\frac{1-\mathrm{i}kR_2}{4\pi R_2^2}\Big]\,\mathrm{e}^{\mathrm{i}kR_2}, \tag{35}$$

where

$$\boldsymbol{u}_s = \big(\sin\mu_p\cos\psi, \sin\mu_p\sin\psi, \cos\mu_p\big). \tag{36}$$

In equation (35), an assumption of $kR_2 \gg 1$ is used such that the parameter $\mathrm{i}kR_2$ is approximated by $(1-\mathrm{i}kR_2)$ in each of the two square bracket terms of the asymptotic formula. These modifications will not cause significant errors in the asymptotic expressions at the far-field, and its introduction can provide a more convenient solution for the total near-field sound pressure given above.

The substitution of equation (35) into equation (8a) leads to a uniform asymptotic solution for the total sound field of

$$p^{(d)}(r, z_s, z) \approx \big(\boldsymbol{l}\cdot\boldsymbol{u}_1\big)\Big[\frac{1-\mathrm{i}kR_1}{4\pi R_1^2}\Big]\,\mathrm{e}^{\mathrm{i}kR_1} + \Big[\big(\boldsymbol{l}\cdot\boldsymbol{u}_2\big)V_\theta + \big(\boldsymbol{l}\cdot\boldsymbol{u}_s\big)\mathrm{Y}_a\Big]\Big[\frac{1-\mathrm{i}kR_2}{4\pi R_2^2}\Big]\,\mathrm{e}^{\mathrm{i}kR_2}, \tag{37a}$$

where V_θ can be identified readily as the plane wave reflection coefficient, which is given by

$$V_\theta = \frac{\cos\theta-\beta_e}{\cos\theta+\beta_e}. \tag{37b}$$

Equation (37a) is the main result of section 2. It offers a closed form analytical formula for rapid computation of sound fields due to an arbitrarily oriented dipole placed above a rigid porous medium. This asymptotic solution will be implemented numerically and compared with other more accurate wave-based numerical solutions. Their validations will be offered in section 5 but the simplified expressions for two special cases will be presented as follows.

An interesting situation arises when the rigid porous medium has a relatively high flow resistivity. In this case, Allard *et al.* [28] suggested that the factor

$$E\sqrt{\sin\theta\sin\mu_p} \approx 1,$$

if both θ and μ_p are close to $\pi/2$. Then, the total sound field can be reduced to

$$p^{(d)}(r, z_s, z) \approx \big(\boldsymbol{l}\cdot\boldsymbol{u}_1\big)\phi_A\Big[\frac{1-\mathrm{i}kR_1}{4\pi R_1^2}\Big]\,\mathrm{e}^{\mathrm{i}kR_1} + \Big[\big(\boldsymbol{l}\cdot\boldsymbol{u}_2\big)V_p + \big(\boldsymbol{l}\cdot\boldsymbol{u}_s\big)\big(1-V_p\big)F(w)\Big]\Big[\frac{1-\mathrm{i}kR_2}{4\pi R_2^2}\Big]\,\mathrm{e}^{\mathrm{i}kR_2}, \tag{38a}$$

where V_p is referred to as the poles of reflection coefficient,

$$V_p = \frac{\cos\theta-\beta_p}{\cos\theta+\beta_p}, \tag{38b}$$

and $F(w)$ is the boundary loss factor calculated by

$$F(w) = 1 + \mathrm{i}\sqrt{\pi}\,w\,\mathrm{e}^{-w^2}\mathrm{erfc}(-\mathrm{i}w), \tag{38c}$$

with the numerical distance w approximated by

$$w \approx \sqrt{\mathrm{i}k_0R_2/2}\big(\cos\theta+\beta_p\big). \tag{38d}$$

In the next special case, we have $n \gg 1$ for a locally reacting ground. Hence, $\beta_e \approx \beta = \zeta n$, which can be interpreted as the specific normalized admittance of the ground surface. Then, it is possible to show that

$$\phi_A \approx \frac{-2\beta}{\cos\theta+\beta}, \tag{39a}$$

$$\phi_B \approx \frac{-2\beta/\sqrt{2\sin\theta\sin\mu_p}}{\sqrt{1-\cos(\mu_p-\theta)}}, \tag{39b}$$

$$\Xi = 2\mathrm{i}\sqrt{\pi}\,\sqrt{\mathrm{i}kR_2/2}\,\beta\,\mathrm{e}^{-w^2}\cdot\mathrm{erfc}(-\mathrm{i}w)/\sqrt{\sin\theta\sin\mu_p}, \tag{40}$$

$$w = \sqrt{2\mathrm{i}kR_2}\sin\big[(\mu_p-\theta)/2\big] \approx \sqrt{\mathrm{i}kR_2/2}\big(\cos\theta+\beta\big), \tag{41a}$$

$$\mu_p = \pi/2 + \arccos\beta, \tag{41b}$$

and

$$V_p \approx V_\theta. \tag{42}$$

Using equations (39)–(42), assuming θ and μ_p are close to $\pi/2$, and taking $\phi_A - \phi_B \approx 0$, we can transform equation (38a) into the same equation derived by Li *et al.* [13], who studied the sound field due to an arbitrarily oriented dipole located above an impedance ground.

3.5. Sound penetration into a rigid porous medium

In an earlier study, Li and Liu showed that the penetration of sound due to an airborne monopole source can be written in terms of the boundary wave term given earlier in equation (1b). The diffracted wave term below the ground can be written in an integral form given in equation (2b). In their analysis for a monopole source, Li and Liu evaluated the integral of equation (2b) asymptotically along the steepest descent path $\overline{C}_\mu$ (see Figure 2). Their solution can be written in an analogous form to yield [6, cf. equation (61)],

$$p_b^{(m)}(r, z_s, -D) = \frac{\mathrm{e}^{\mathrm{i}kL}}{4\pi\Delta}\Big[2 + 2\mathrm{i}\sqrt{\pi}\sqrt{\mathrm{i}kR_r/2}\cdot\frac{\beta_p\,\mathrm{e}^{-\bar{w}^2}\mathrm{erfc}(-\mathrm{i}\bar{w})}{(1-\zeta^2)\sqrt{\sin\vartheta\sin\mu_p}} + \overline{\phi}^{(m)}\Big], \tag{43}$$

where $D > 0$ is the depth below the interface, the overbar represents the corresponding parameters in the rigid porous medium, L is the acoustical path length and Δ is the physical path length where

$$L = f_b(\vartheta) = R_s + nR_D \tag{44a}$$

and

$$\Delta = \sqrt{\overline{R}_2 R_r}. \tag{44b}$$

The separations between the source and the receiver, R_s and R_D, are respectively given by

$$R_s = z/\cos\vartheta \tag{45a}$$

and

$$R_D = D/\cos\vartheta_1. \tag{45b}$$

In equations (43) and (44b), the apparent distance of the sound ray traveling in the absence of the lower medium, which is denoted by $\overline{R}_2$, is defined as

$$\overline{R}_2 = r/\sin\vartheta \tag{46a}$$

and the acoustical energy path length [25] R_r is calculated by

$$R_r = R_s + /R_D/n)(\cos\vartheta/\cos\vartheta_1)^2, \tag{46b}$$

where ϑ is the incident angle and ϑ_1 is the refracted angle. These two angles are related according to Snell's Law, i.e. $\sin\vartheta = n\sin\vartheta_1$. The representations of these physically interpretable parameters are shown in Figure 1. Li and Liu [6] outlined a simple numerical scheme to determine ϑ and ϑ_1 numerically for a given source/receiver configuration and the acoustical characteristic of the ground surface.

In equation (43), the numerical distance of the refracted wave $\bar{w}$ is given by [29],

$$\bar{w} = \sqrt{\mathrm{i}k}\sqrt{L - R_s\cos(\mu_p - \vartheta) - nR_D\cos(\mu_{p1} - \vartheta_1)}, \tag{47}$$

where μ_p and μ_{p1} is the pole in the respective complex μ-plane and μ_1-plane. Again, these two angles are related according to the Snell Law, i.e., $\sin\mu_p = n\sin\mu_{p1}$. Furthermore, the correction factor $\overline{\phi}^{(m)}$ in equation (43) can be written in a familiar form as

$$\overline{\phi}^{(m)} = \overline{\phi}_A - \overline{\phi}_B. \tag{48a}$$

where

$$\overline{\phi}_A \approx \frac{-2\beta_\vartheta}{\cos\theta + \beta_\vartheta}, \tag{48b}$$

$$\overline{\phi}_B \approx \frac{-2\beta_p/\sqrt{2\sin\vartheta\sin\mu_p}}{(1-\zeta^2)\sqrt{1-\cos(\mu_p - \vartheta)}}, \tag{48c}$$

and the effective admittance β_ϑ of the rigid porous medium is given by

$$\beta_\vartheta = \zeta\sqrt{n^2 - \sin^2\vartheta}. \tag{48d}$$

In light of the analysis shown in the appendix, it is possible to rewrite the diffracted wave term below the rigid porous medium, i.e., equation (43), in a comparable form as

$$p_b^{(m)} = \frac{\mathrm{e}^{\mathrm{i}kL}}{4\pi\Delta}\left[T_\vartheta + \mathrm{Y}_b\right] \tag{49a}$$

where the plane wave transmission coefficient can be defined as

$$T_\vartheta = 2 + \overline{\phi}_A = 2\cos\vartheta/(\cos\vartheta + \beta_\vartheta), \tag{49b}$$

the diffraction factor below the ground is given by

$$\mathrm{Y}_b = \bar{\Xi} - \overline{\phi}_B, \tag{49c}$$

and the variable $\bar{\Xi}$, cf equation (18), can be calculated by

$$\bar{\Xi} = 2\mathrm{i}\sqrt{\pi}\sqrt{\mathrm{i}kR_2/2}\frac{\beta_p\,\mathrm{e}^{-w^2}\,\mathrm{erfc}(-\mathrm{i}\bar{w})}{(1-\zeta^2)\sqrt{\sin\theta\sin\mu_p}}. \tag{49d}$$

By noting equation (4), it is possible to write the dipole sound field below the porous ground in terms of $p_b^{(d)}$ as

$$p_b^{(d)} = \sin\gamma_L\cos(\psi - \psi_L)\frac{\partial p_b^{(m)}}{\partial r_s} + \cos\gamma_L\frac{\partial p_b^{(m)}}{\partial z_s}, \tag{50}$$

where the first term is the sound field due to the horizontal dipole and the second term is that due to the vertical dipole. Using the expression in equation (2b) for $p_b^{(m)}$, we can write the horizontal and vertical dipole terms in the respective integral forms as

$$\begin{aligned}\partial_r p_b^{(m)} &= \frac{\partial p_b^{(m)}}{\partial r} \\ &= \frac{\mathrm{i}k^2}{4\pi}\int_C \frac{\cos\mu\sin\mu\,G_1(\mu)\exp[\mathrm{i}k f_b(\mu)]}{\cos\mu + \zeta\,N(\mu)}\,\mathrm{d}\mu,\end{aligned} \tag{51a}$$

and

$$\begin{aligned}\partial_z p_b^{(m)} &= \frac{\partial p_b^{(m)}}{\partial z} \\ &= \frac{k^2}{4\pi}\int_C \frac{\cos^2\mu\,G_0(\mu)\exp[\mathrm{i}k f_b(\mu)]}{\cos\mu + \zeta\,N(\mu)}\,\mathrm{d}\mu.\end{aligned} \tag{51b}$$

Using the same procedures as described in section 3, equations (51a) and (51b) can be evaluated asymptotically to yield

$$\begin{aligned}\partial_r p_b^{(m)} = \mathrm{i}k\big[&2\sin\vartheta + \bar{\Xi}\sin\mu_p \\ &+ \overline{\phi}_A\sin\vartheta - \overline{\phi}_B\sin\mu_p\big]\mathrm{e}^{\mathrm{i}kL}/(4\pi\Delta)\end{aligned} \tag{52a}$$

and

$$\begin{aligned}\partial_z p_b^{(m)} = \mathrm{i}k\big[&2\cos\vartheta + \bar{\Xi}\cos\mu_p \\ &+ \overline{\phi}_A\cos\vartheta - \overline{\phi}_B\cos\mu_p\big]\mathrm{e}^{\mathrm{i}kL}/(4\pi\Delta).\end{aligned} \tag{52b}$$

Noting equation (37a), it is useful to derive a comparable expression for the sound field below the ground. The

dipole sound pressure can be obtained by an alternative approach

$$\partial_r p_b^{(m)} = \frac{\partial}{\partial r}\left[p_b^{(m)}\right], \qquad \partial_z p_b^{(m)} = \frac{\partial}{\partial z}\left[p_b^{(m)}\right]. \tag{53}$$

The respective near-field components can then be derived to yield

$$\partial_r p_b^{(m)} \approx -\frac{[T_\vartheta + \mathrm{Y}_b]\mathrm{e}^{\mathrm{i}kL}}{4\pi\Delta^2}\frac{\partial\Delta}{\partial r} \tag{54a}$$

and

$$\partial_z p_b^{(m)} \approx -\frac{[T_\vartheta + \mathrm{Y}_b]\mathrm{e}^{\mathrm{i}kL}}{4\pi\Delta^2}\frac{\partial\Delta}{\partial z}, \tag{54b}$$

where only the $(1/\Delta^2)$ term remains in the above equations when $r \to 0$, i.e., $\vartheta \approx \vartheta_1 \approx 0$. It then follows from equation (44a) that the acoustical energy path length can be approximated by $R_r \approx r/\sin\vartheta = \overline{R}_2$. Thus, the physical length (see equation 44b) can be reduced to $\Delta \approx r/\sin\vartheta = \overline{R}_2$. Consequently, it can be easily shown that

$$\partial\Delta/\partial r \approx \sin\vartheta, \qquad \partial\Delta/\partial z \approx \cos\vartheta \tag{55}$$

at the near-field.

By matching equations (54a) and (54b) with the corresponding asymptotic solution given in equations (52a) and (52b), we can establish a generalized solution that is both accurate at the near- field and far-field as follows. For the sound field due to a horizontal dipole, the asymptotic solution is given by

$$\begin{aligned}\partial_r p_b^{(m)} &= -T_\vartheta \sin\vartheta\left[\frac{1-\mathrm{i}k\Delta}{4\pi\Delta^2}\right]\mathrm{e}^{\mathrm{i}kL} \\ &\quad - \mathrm{Y}_b\left[\frac{\sin\vartheta - \mathrm{i}k\Delta\sin\mu_p}{4\pi\Delta^2}\right]\mathrm{e}^{\mathrm{i}kL}.\end{aligned} \tag{56a}$$

For a vertical dipole, the sound field is expressed as

$$\begin{aligned}\partial_z p_b^{(m)} &= -T_\vartheta \cos\vartheta\left[\frac{1-\mathrm{i}k\Delta}{4\pi\Delta^2}\right]\mathrm{e}^{\mathrm{i}kL} \\ &\quad - \mathrm{Y}_b\left[\frac{\cos\vartheta - \mathrm{i}k\Delta\cos\mu_p}{4\pi\Delta^2}\right]\mathrm{e}^{\mathrm{i}kL}.\end{aligned} \tag{56b}$$

Substituting equations (56a) and (56b) into equation (50) and assuming $k\Delta \gg 1$, we can obtain an asymptotic expression for the dipole sound field below the ground as

$$\begin{aligned}p_p^{(d)}(r, z_s, -D) &= \left(\boldsymbol{l}\cdot\bar{\boldsymbol{u}}_2\right)T_\vartheta\left[\frac{1-\mathrm{i}k\Delta}{4\pi\Delta^2}\right]\mathrm{e}^{\mathrm{i}kL} \\ &\quad + \mathrm{Y}_b\left[\frac{\left(\boldsymbol{l}\cdot\bar{\boldsymbol{u}}_2\right) - \mathrm{i}k\left(\boldsymbol{l}\cdot\boldsymbol{u}_s\right)\Delta}{4\pi\Delta^2}\right]\mathrm{e}^{\mathrm{i}kL},\end{aligned} \tag{57}$$

where $\bar{\boldsymbol{u}}_2$ and $\boldsymbol{u}_s$ are the unit vectors that characterize the direction of the transmitted wave and the boundary wave propagation, respectively. The unit vector $\bar{\boldsymbol{u}}_2$ is given by

$$\bar{\boldsymbol{u}}_2 = \big/\sin\vartheta\cos\psi, \sin\vartheta\sin\psi, \cos\vartheta\big) \tag{58}$$

and $\boldsymbol{u}_s$ defined in equation (36).

Equation (57) presents an analytical solution for predicting sound penetration into porous ground due to an arbitrarily oriented dipole source. This asymptotic formula, which has not been published elsewhere, is the main result of this section. The validity of equation (57) will be confirmed in section 5 below.

3.6. Validation of asymptotic formulas

The asymptotic formulas derived in the last section can be used to efficiently calculate the sound fields due to an arbitrarily oriented dipole. For the present study, it is sufficient to use a simple empirical model for modeling the acoustical characteristics of the ground surfaces. According to Miki [30], the normalized characteristic impedance Z_c and the index of refraction (propagation constant) are given as

$$\begin{aligned}Z_c &= \rho_1 c_1/\rho c \\ &= (q/\Omega)\left[1 + 0.07(\sigma_e/f)^{0.632} + 0.107\mathrm{i}(\sigma_e/f)^{0.632}\right],\end{aligned} \tag{59a}$$

and

$$n = q\left[1 + 0.109(\sigma_e/f)^{0.618} + 0.160\mathrm{i}(\sigma_e/f)^{0.618}\right], \tag{59b}$$

where q is the tortuosity, Ω is the porosity, σ_e is the effective flow resistivity of the porous medium, and f is the frequency of the acoustic disturbances. The density ratio can then be derived from equations (59a) and (59b) to yield

$$\zeta = \frac{\Omega\left[1 + 0.07(\sigma_e/f)^{0.632} + 0.107\mathrm{i}(\sigma_e/f)^{0.632}\right]^{-1}}{q^2\left[1 + 0.109(\sigma_e/f)^{0.618} + 0.160\mathrm{i}(\sigma_e/f)^{0.618}\right]}. \tag{59c}$$

In the determination of Z_c, n, and ζ, the effective flow resistivity is used instead of the flow resistivity, σ_p. These two parameters, σ_e and σ_f, are related by

$$\sigma_e = \frac{s_f^2\Omega}{q^2}\sigma_p, \tag{60}$$

where s_f is the pore shape factor. It is remarkable that q, Ω, s_f, and σ_p are identical parameters used by Attenborough for the classical four-parameter impedance model [31]. Here, the Miki empirical model only requires three independent parameters, which are σ_e, q, and Ω.

The numerical solutions computed by the asymptotic formulas are compared with the exact numerical solutions calculated by a combination of the fast field program (FFP) and the direct numerical integration method in the wave number space. This exact computation scheme is referred to as the integrated exact solution (IES) in the following paragraphs. To present the numerical results, an excess attenuation function is used, which is defined as

$$EA(G_\beta) = 20\log_{10}\left[\frac{G_\beta}{\mathrm{e}^{\mathrm{i}kr}/4\pi r}\right], \tag{61}$$

and G_β is the function of interest that can be the diffracted wave terms for the horizontal dipole placed above and below the rigid porous medium, i.e., $\partial_r p_a^{(m)}$ and $\partial_r p_b^{(m)}$. It can

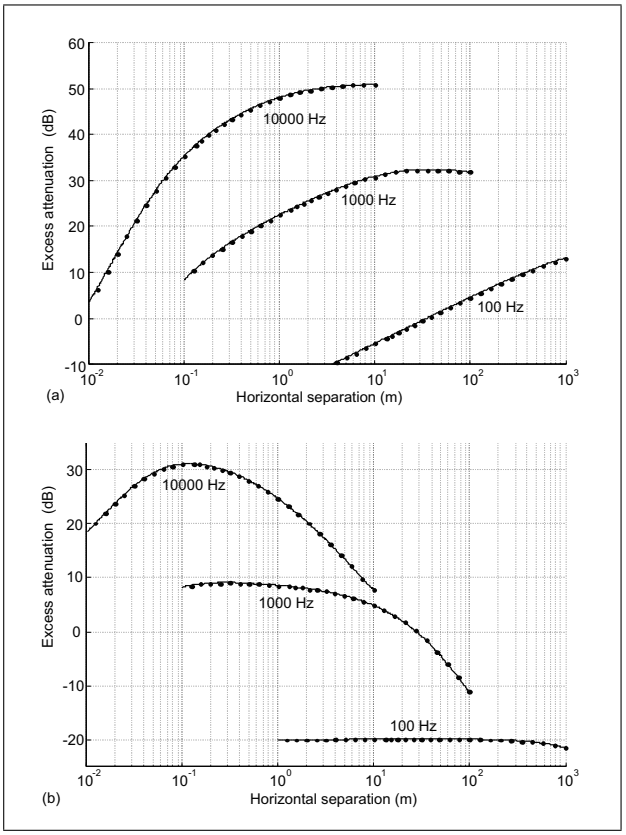


Figure 3. Predicted excess attenuation of the diffracted wave term against horizontal separation for the receiver located 0.02 m above the ground and source located 0.04 m above the ground: (a) a horizontal dipole; (b) a vertical dipole. The Miki empirical model was used for the porous layer with an effective flow resistivity of 50 kPa s/m^2, tortuosity of 1.1, and porosity of 0.9. Solid line: asymptotic formulas. Circles: Integrated exact solution (IES).

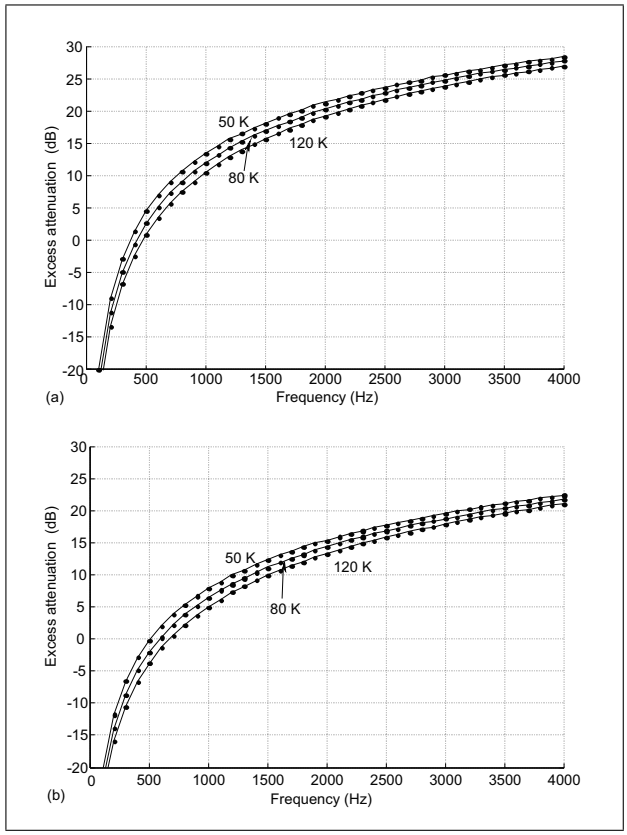


Figure 4. (a): Predicted excess attenuation spectrum of the diffracted wave term for the receiver located 0.3 m above the ground, source located 0.2 m above the ground, and a horizontal separation of 1 m: (a) a horizontal dipole; (b) a vertical dipole. The Miki empirical model was used for the porous layer with effective flow resistivities of 50 kPa s/m^2, 80 kPa s/m^2, and 120 kPa s/m^2, tortuosity of 1.1, and porosity of 0.9. Solid line: the asymptotic formulas. Circles: Integrated exact solution (IES).

also be used to represent the respective diffracted wave terms (above and below the ground) due to the vertical dipole, which are $\partial_z p_a^{(m)}$ and $\partial_z p_b^{(m)}$, respectively.

Extensive computations have been conducted for a series of source/receiver geometries and for a wide range of ground surfaces. It is found that all the numerical results based on the asymptotic formulas agree well (to within about 0.5 dB) with the IES when $kr \sim 1$. The agreements are generally even better for large values of kr (to within 0.1 dB). Unless stated otherwise, the parametric values of 50 kPa s/m^2, 1.1, and 0.9 were selected for the effective flow resistivity (σ_e), tortuosity (q) and porosity (Ω), respectively, in all the numerical simulations. They represent typical values for a rigid porous interface. It is possible to use the asymptotic formula due to an arbitrarily oriented dipole for comparison with the IES. However, it is more convenient to separately validate each of the asymptotic formulas for the horizontal and vertical dipoles.

First, we present the numerical results for the dipole sound fields above a rigid porous medium. Figures 3a and 3b show the comparisons of the diffracted wave terms due to a horizontal dipole and a vertical dipole, respectively. The corresponding excess attenuation functions, see equation (61), are plotted against the horizontal separation r. The numerical results for frequencies at 100 Hz (low), 1 kHz (mid), and 10 kHz (high) are shown in these two plots. We found that the diffracted wave terms became more critical when the source and receiver was close to the ground surface. Hence, the source and receiver were respectively chosen at 0.04 m and 0.02 m above the ground surface to highlight the accuracy of the asymptotic formulas in these presentations. Generally, the predictions according to the asymptotic formulas agreed very well with those predicted by the IES, provided that kR_2 is greater than approximately 1, which may be treated as a heuristic condition for the asymptotic formulas.

Figures 4a and 4b display the corresponding EA spectra for the horizontal dipole and vertical dipole. In these two plots, the source and receiver remained at 0.04 m and 0.02 m above the ground but the horizontal range was set at 1 m. In addition, we also show the predicted results for different values of σ_e at 50, 80, and 120 kPa s/m^2; however, q and Ω were set constant at 1.1 and 0.9, respectively. Excellent agreements are shown in these two EA spectra for the respective diffracted wave terms above the rigid porous medium due to the horizontal and vertical dipoles.

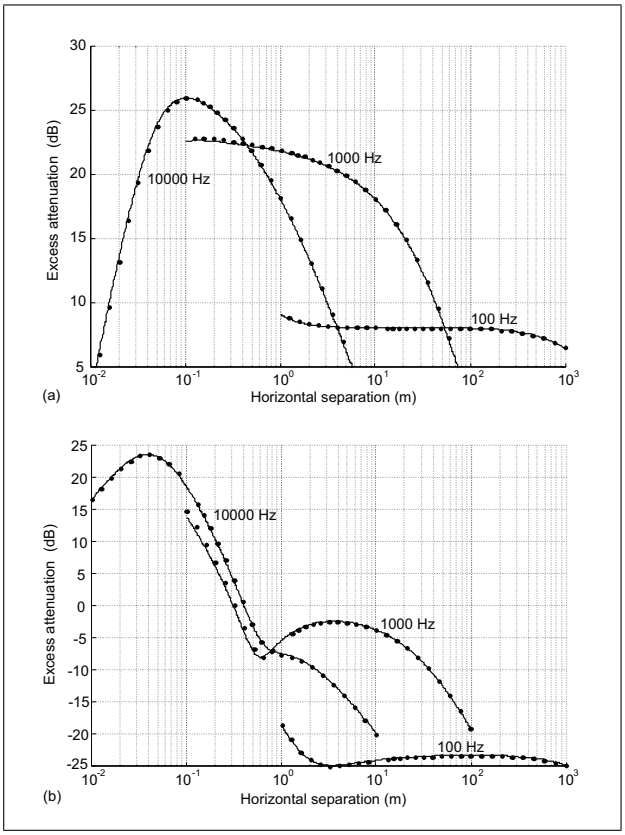


Figure 5. Predicted excess attenuation of the diffracted wave terms is plotted against the horizontal separation: (a) a horizontal dipole; (b) a vertical dipole. The ground parameters and other captions are the same as for Figure 3 except that the receiver is located 0.02 m below the ground.

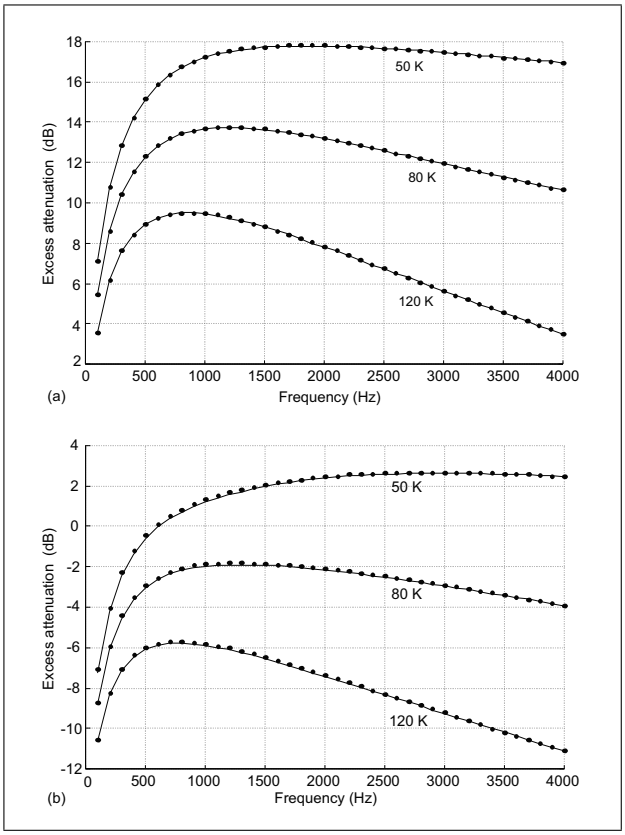


Figure 6. Predicted excess attenuation spectrum for (a) a horizontal dipole; (b) a vertical dipole. The parameters and other captions are the same as for Figure 4 except that the receiver is located 0.03 m below the ground.

In the next two sets of figures, we show the validation of the asymptotic formulas for the prediction of the dipole sound fields below the air/ground interface. Because there was no direct wave term as the interface shielded the direct line of sight between the source and receiver, the diffracted wave term represented the total sound field in each of the respective situations for the horizontal and vertical dipoles.

Figures 5a and 5b are the numerical results for the diffracted wave terms plotted against the horizontal range. The same type of ground surfaces were used in the simulations, which were identical to those used in Figures 3a and 3b. However, in Figures 5a and 5b, the source was located at the same height of 0.04 m above the air/ground interface but the receiver was located 0.02 m below the interface. The acoustical characteristics of the ground surface used were the same as those used for the simulations for Figures 4a and 4b. With the matched asymptotic solutions, we can see that both formulas agreed very well with the predictions according to the IES, provided that kR_2 was greater than approximately 1. Figures 6a and 6b are the corresponding EA spectra for the sound fields due to the horizontal dipole and the vertical dipole, respectively. In this set of simulations, the source was located 0.2 m above ground but the receiver was situated 0.03 m below the interface. The horizontal separation between the source and receiver was 1 m. As shown in this set of figures, the agreements between the asymptotic solutions and the IES were reasonably good.

It is of interest to point out that the IES method is based on the summation of the contributions from a large number of sampling points in order to achieve the required accuracy in the calculation of the sound fields. For instance, a total of about 400,000 sampling points is typically needed for a source frequency of 10 kHz and a source/receiver separation of 100 m. On the other hand, the calculations of the asymptotic sound fields can usually be achieved in real time at all frequencies.

4. Conclusion

The asymptotic formulas developed here provide an efficient means for calculating the sound fields due to an arbitrarily oriented dipole placed above a rigid porous medium. There are separate analytic formulas to predict the contributions from the diffracted wave terms accounting for the sound reflected from and transmitted through a fluid-fluid interface. The validity of these asymptotic formulas has been confirmed by comparison with an accurate, but computational intensive wave-based numerical scheme. The asymptotic solutions can be applied in the

boundary element formulation by providing an appropriate Green's function for modeling a more complex environment with the presence of non-locally reacting sound absorbing materials.

Appendix

Appendix: Diffracted wave fields and total sound fields due to monopole

Li and Liu [7] showed that the diffracted wave term $p_a^{(m)}$ due to the monopole source can be evaluated asymptotically to yield a sum of the main term Ξ and its correction factor $\phi^{(m)}$,

$$p_a^{(d)} = \left[\Xi + \phi^{(m)}\right] \frac{e^{ikR_2}}{4\pi R_2} \tag{A1a}$$

where Ξ is dependent on the complimentary error function term defined by equation (18) and the correction term is specified by

$$\phi^{(m)} = \phi_A - \phi_B, \tag{A1b}$$

with ϕ_A and ϕ_B given in equations (20a) and (22b), respectively. By taking inspiration from the form of solutions for a diffracted wave term for the dipole source, it is possible to express the diffracted wave term of the monopole sound fields by

$$p_a^{(m)} = \left[\phi_A + \mathrm{Y}_a\right] \frac{e^{ikR_2}}{4\pi R_2}, \tag{A2}$$

where the diffraction factor Y_a is defined by equation (24b). The substitution of equation (A2) into equation (3a) leads to an asymptotic expression for the total sound field,

$$p^{(m)} = \frac{e^{ikR_1}}{4\pi R_1} + \left[V_\theta + \mathrm{Y}_a\right] \frac{e^{ikR_2}}{4\pi R_2}. \tag{A3}$$

This expression provides a better physical insight of the asymptotic solution given above. The first term of equation (A3) is the direct wave term and the second term is the reflected wave term. There are two components for the reflected wave term: the first component in the curly bracket of equation (A3) is the plane wave reflection term, and the second component is the diffraction factor. The second term vanishes when the value of w is high, i.e., a condition when the plane wave term is sufficient for representing the reflected wave term. A re-examination of equation (38a) suggests that the same interpretation holds true for the sound field due to an arbitrarily oriented dipole, although extra factors, $(\boldsymbol{l}\cdot\boldsymbol{u}_1)$, $(\boldsymbol{l}\cdot\boldsymbol{u}_2)$ and $(\boldsymbol{l}\cdot\boldsymbol{u}_s)$, are needed to account for the source orientation relative to the receiver location. These interpretations facilitate the development of the asymptotic formula for sound penetration into the porous ground given in section 4 in the main text.

Acknowledgement

One of the authors (HT) gratefully acknowledges the China Scholarship Council (CRC) of the National Science Foundation for financial supports.

References

[1] U. Ingard: On the reflection of a spherical sound wave from an infinite plane. J. Acoust. Soc. Am. **23** (1951) 329–335.

[2] R. B. Lawhead, I. Rudnick: Acoustic wave propagation along a constant normal impedance boundary. J. Acoust. Soc. Am. **23** (1951) 546–549.

[3] D. I. Paul: Acoustical radiation from a point source in the presence of two media. J. Acoust. Soc. Am. **29** (1957) 1102–1109.

[4] M. Briquet, P. Fillippi: Diffraction of a spherical wave by absorbing plane. J. Acoust. Soc. Am. **61** (1977) 640–646.

[5] P. J. T. Filippi, D. Habault: Reflection of a spherical wave by the plane interface between a perfect fluid and a porous medium. J. Sound Vib. **56** (1978) 97–103.

[6] K. Attenborough, S. I. Hayek, J. M. Lawther: Propagation of sound over a porous half-space. J. Acoust. Soc. Am. **65** (1980) 1493–1501.

[7] K. M. Li, S. Liu: Fast asymptotic solutions for sound fields above and below a rigid porous ground. J. Acoust. Soc. Am. **130** (2011) 1103–1114.

[8] G. Kristensson, S. Ström: Scattering from buried inhomogeneities – a general three-dimensional formalism. J. Acoust. Soc. Am. **64** (1978) 917–936.

[9] D. L. Berry, S. N. Chandler Wilde, K. Attenborough: Acoustic scattering by a near surface obstacle in a rigid porous medium. J. Sound Vib. **170** (1994) 161–179.

[10] C. G. Don, A. J. Rogers: Using acoustic impulses to identify a buried nonmetallic object. J. Acoust. Soc. Am. **95** (1994) 2837–2838.

[11] D. Velea, R. Waxler, J. M. Sabatier: An effective fluid model for landmine detection using acoustic to seismic coupling. J. Acoust. Soc. Am. **115** (2004) 1993–2000.

[12] O. Zaporozhets, V. Tokarev, K. Attenborough: Predicting noise from aircraft operated on the ground. Appl. Acoust. **64** (2003) 941–953.

[13] Z. Hu, J. S. Bolton: Sound propagation from an arbitrarily multi-pole placed near a plane finite impedance surface. J. Sound Vib. **170** (1994) 637–666.

[14] K. M. Li, S. Taherzadeh, K. Attenborough: Sound propagation from a dipole source near an impedance plane. J. Acoust. Soc. Am. **101** (1997) 3343–3352.

[15] P. Menounou, E. S. Papaefthymiou: Shadowing of directional noise sources by finite noise barriers. Appl. Acoust. **71** (2010) 351–367.

[16] S. Peters: The prediction of railway noise profiles. J. Sound Vib. **32** (1972) 87–99.

[17] K. S. Bretner, F. Farassat: Helicopter noise prediction: the current status and future directions. J. Sound Vib. **170** (1994) 79–96.

[18] A. Banos: Dipole radiation in the presence of a conducting half-space, 1st ed. Pergamon Press, Oxford, 1966.

[19] R. W. P. King: The electromagnetic field of a vertical dipole over the earth or sea. IEEE Trans. Ant. Prog. **42** (2004) 382–389.

[20] T. Fei, L. W. Li, T. S. Yeo, H. L. Wang, Q. Wu: A comparable study of radio wave propagation over the earth due to a vertical electric dipole. IEEE Trans. Ant. Prog. **55** (2007) 2723–2732.

[21] T. L. Richards, K. Attenborough: Accurate FFT-based Hankel transform for predictions of outdoor sound propagation. J. Sound Vib. **109** (1986) 157–167.

[22] M. Boue, H. Boden, I. Karasalo: Outdoor sound propagation using an exact finite element method. AIAA Paper 2001-2261, 2001.

[23] K. M. Li: An analytical formulation for predicting the attenuation of sound in a porous ground from an airborne source. J. Acoust. Soc. Am. **123** (2008) 1352–1363.

[24] C. F. Chien, W. W. Soroka: Sound propagation along an impedance plane. J. Sound Vib. **43** (1975) 9–20.

[25] L. M. Brekhovskik: Waves in layered media. Ch. 4, 2nd ed. Academic Press, New York, 1980.

[26] F. Anfosso-Ledee, P. Dangla, M. Beregier: Sound propagation above a porous road surface with extended reaction by boundary element method. J. Acoust. Soc. Am. **122** (2007) 731–736.

[27] M. Abramowitz, I. A. Stegun: Handbook of mathematical functions with formulas, graphs and mathematical tables. Ch. 7 and Ch. 9. Dover Publications, Inc., New York, 1972.

[28] J. F. Allard, G. Jansens, W. Lauriks: Reflection of spherical waves by non-locally reacting media. Wave Motion **36** (2002) 143–155.

[29] There are two notable typographical errors in equations (21b) and (60a) of [7]. they are corrected, respectively, here in equations (5b) and (47).

[30] Y. Miki: Acoustical properties of porous materials. Generalizations of empirical models. J. Acoust. Soc. Jpn. (E) **11** (1990) 25–28.

[31] K. Attenborough: Acoustical characteristics of rigid fibrous absorbents and granular materials. J. Acoust. Soc. Am. **73** (983) 785–799.